Hindawi
Wireless Communications and Mobile Computing
Volume 2019, Article ID 9767404, 13 pages
https://doi.org/10.1155/2019/9767404

Research Article

Tool for Recovering after Meteorological Events Using a Real-Time REM and IoT Management Platform

Yosvany Hervis Santana,[1,2] **David Plets**,[1] **Rodney Martinez Alonso**,[1,2] **Glauco A. Guillen Nieto**,[2] **Nasiel Garcia Fernandez**,[2] **Margot Deruyck**,[1] **and Wout Joseph**[1]

[1]*Information Technology, Ghent University-IMEC, Ghent 9052, Belgium*
[2]*R&D Telecom, LACETEL, Havana 19200, Cuba*

Correspondence should be addressed to Yosvany Hervis Santana; yosvany.hervissantana@ugent.be

Received 28 March 2019; Revised 14 June 2019; Accepted 24 June 2019; Published 9 July 2019

Guest Editor: Maurizio Casoni

This paper is the design of a Radio Environment Map (REM) with a real-time tool to sense the radiofrequency spectrum and optimally places with Surrogate Modelling and Sequential Experimental Design tools a total of 72 SDR sensors in the selected area, using LoRa and/or NB-IoT technologies for networking. It permits the regulatory body to check the correct use of the assigned spectrum and constitutes a communication alternative in case of a catastrophic event, such as a hurricane or an earthquake, where radio and TV broadcasting play an important role in keeping people informed after such meteorological event. The radiobroadcast services use large antennas and high towers, making them vulnerable to such events. Regardless of the chosen technology, the IoT monitoring network will be more robust, since it uses small antennas and lower towers, and often a given area is covered by multiple base stations. The tool can be used to deploy new services in the nonserved area (e.g., 4G in the 700 MHz band at a lower cost or using TVWS techniques to provide communications and internet connection) and optimal interference management.

1. Introduction

Wireless communications and broadcasting play a vital role in connecting people around the world. These systems are used to inform, entertain, educate, and protect citizens. However, in developing countries, financial resources are not always available to have them operate efficiently.

Many developed countries introduce new broadband services, e.g., fourth-generation networks (4G), at higher frequencies (Long Term Evolution, LTE) band 38, 2570 MHz-2620 MHz). However, at higher frequencies, base stations will have a reduced coverage area, requiring much more base stations for the same service area. This densification of base stations is not feasible in underdeveloped countries because of the high cost. Moving these services to lower frequencies (e.g., 700 MHz) the numbers of base stations will be lower covering more area.

Some underdeveloped countries deploy their network in a progressive way based in coverage area without any planning tool. The major unsolved issue in efficiently sharing radio frequency spectrum between different services is related to the coverage area and radiated power by base stations.

Spectrum sensing performed by Cognitive Radio (CR) seems adequate due to its lower infrastructure requirement and wide application areas [1, 2]. In the case of CR, the spectrum-sensing task is to obtain the characteristics of spectrum usage. Moreover, it determines the type of signals that occupy the spectrum (digital or analog signals) and their features like the waveform, modulation, carrier frequency, and bandwidth, among others. However, this needs more precise signal analysis techniques which adds computational complexity to the detection algorithms [3].

CRs can avoid interference with primary users. Reliable sensing techniques identify the possible availability of spectrum opportunities to increase dynamic access to cognitive networks capacity. The most valuable parameters of the CR concept are the ability to sense, detect, learn, and be

aware of the radio operating environment, the state of the communication channel, the spectrum availability, the user requirements and applications, the local policies, the available networks (infrastructures), and the operating restrictions determined by the regulatory body. But the principal feature is its capacity of flexible autonomous autoreconfiguration [4].

Software Defined Radio (SDR) is one of the most significant and latest technologies already and profusely commercially in use for modern wireless communication-related systems. SDR, the hardware platform of almost all CR, can tune different frequency ranges and implement various (de-)modulation schemes and various standards in the same device/hardware by using a reconfigurable hardware and software system [5]. In SDR, a broader range of capabilities depends on elements which are basically software configurable [6]. The two major advantages of SDR are flexibility and easy adaptation. However, the deployments of SDR sensors technology with the capability of transmitting information are usually expensive [7]. Most recent advances on standardization and industrialization for the Internet of Things (IoT) technologies could contribute to solving the interconnection of the SDR devices.

Cuba is yearly hit by tropical storms (e.g., hurricane Irma in 2017) causing a lot of damage in the telecommunications infrastructure, destroying people's houses and making the circulation impossible. In this case, the recovery process should have good synchronization among the involved entities. Regardless of the chosen technology, the IoT monitoring network (using SDR sensors as sensing devices) will be more robust, since it uses small antennas and lower towers and often a given area is covered by multiple base stations. Having a Dynamic Monitoring Tool (DMT) able to detect in real time the radiofrequency spectrum and making suggestions with possible solutions is helpful to cover the damaged zone by the hurricane and keep the people informed.

The novelty of this paper is the design of a tool that senses and monitors in real time the radiofrequency spectrum and optimally places with Surrogate Modelling (SUMO) and Sequential Experimental Design (SED) tools a number of SDR sensors in the selected area, using LoRa and/or NB-IoT technologies for networking [1]. This tool will build a REM of the selected radiofrequency spectrum and use this information for the following purposes. First, it permits the regulatory body to check the correct use of the assigned spectrum. Second, it constitutes an alternative during recovery process in case of a catastrophic event, such as a hurricane or an earthquake, where radio and TV broadcasting play an important role in keeping people informed. The radiobroadcast services use large antennas and high towers, making them vulnerable to such events. Third, the tool will be useful for decision-making authorities and service providers, showing the real-time available frequencies and coverage interference about nonserved or underserved areas because of the damage caused by the event. Fourth, the tool can be used to deploy new services in the nonserved area (e.g., 4G in the 700 MHz band at a lower cost or using TVWS techniques to provide communications and internet connection).

This paper continues as follows. Section 2 presents the related work and the IoT platform solution. Section 3 proposes a network's architecture for our system. A real broadcasting scenario is considered, including the optimization for sensor position and IoT base stations. Section 4 shows the results for the network design, the feedback loop for different IoT platforms, and spectrum usage efficiency. Conclusions are presented in Section 5.

2. Related Work and IoT Platform Solutions

2.1. Related Work. A surrogate model is a cheap-to-evaluate replacement model of expensive, highly accurate computer simulations (e.g., sensors positioning). Hence, the SUrrogate MOdeling and Sequential Design tools are an alternative to deeply explore the design space by evaluating large amounts of samples. In [8], the authors use a surrogate model to simulate the behavior of RF circuits. In [9], the same authors use a surrogate model to find the best approximation of a LNA describing functions.

Using SED, all the data points are chosen at once and the modelling algorithm proceeds from there, without evaluating any additional samples later. In [10], the authors present a comparison and analysis of different space-filling sequential design methods, where the results are compared to traditional one-shot Latin hypercube designs. In [11], a comparison is made among different Sequential Experimental Design methods for global surrogate modeling on a real-world electronics problem.

Spectrum sensing, as a key enabling functionality in CRNs, needs to reliably detect weak Primary Radio (PR) signals of possibly unknown device types [4]. Spectrum sensing should also monitor the activation of primary users to vacate the occupied spectrum segments for secondary users. However, it is difficult for CR to capture such information instantaneously due to the absence of cooperation between the primary and secondary users. Recent research efforts on spectrum sensing have focused on the detection of ongoing primary transmissions by CR devices. Generally, spectrum-sensing techniques fall into two categories: wideband sensing and narrowband sense. Narrowband sensing splits coherent [12] and noncoherent detection. For coherent detection, no knowledge about the parameters of the primary signal is required, while noncoherent detection is the most appropriate one when the SDR has limited information on the primary signals (e.g., only the local noise power is known) [13]. Energy detector [14] is an example of noncoherent detection, while the waveform detector and the cyclostationary detector are coherent [3].

Collecting measurements for constructing the REM can be done by SDRs. Therefore, developing dedicated sensors to increase the quality of the REM must be considered. In [16], the effect of sensor geometries on Primary Users (PU) and the environmental parameter estimation are studied. Distributed spectrum sensing with Cognitive Radio Networks (CRNs) by exploiting sparsity is proposed in [17].

To obtain knowledge about the network, a generic approach to develop CR based on the REM is proposed in [18,

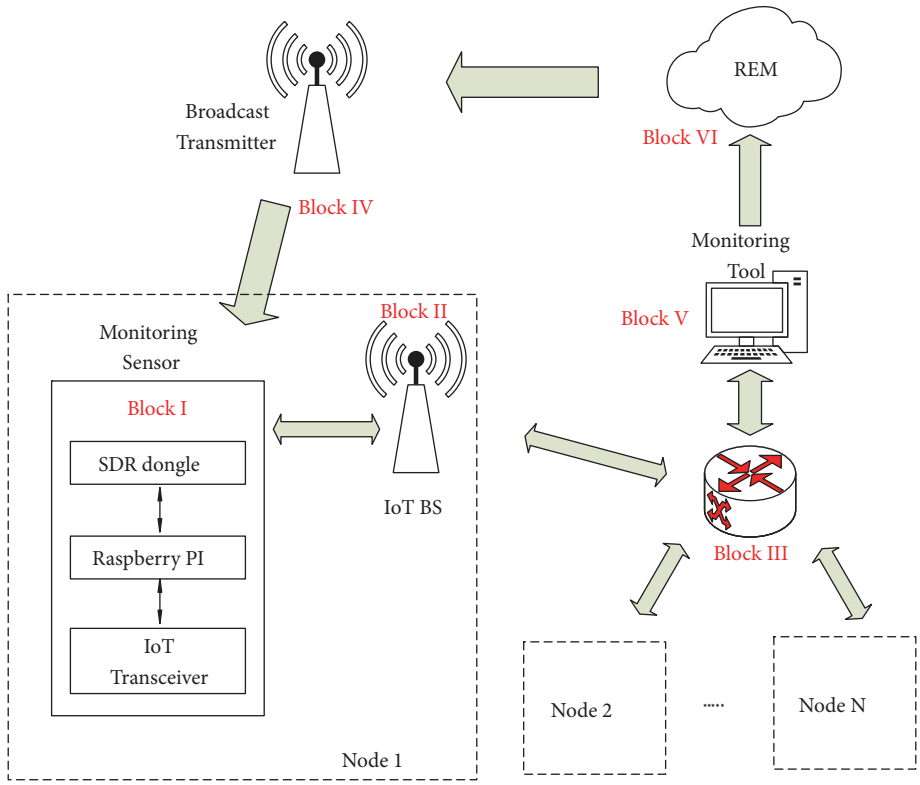

Figure 1: Dynamic network architecture.

19]. A REM is envisioned as an integrated database consisting of multidomain information, which supports global cross-layer optimization by enabling CR to "look" through various layers. The cognitive radio engine (CE) for various cognitive functionalities such as situation awareness, reasoning, learning, planning, and decision support can exploit the REM, as a vehicle of network support to CR. In [18], simulation results are presented. However, the authors do not consider different metrics for performance evaluation (e.g., the environmental noise interferences produced by cars, weather, and adjacent transmitters).

2.2. IoT Platform Solution. In recent years, IoT networks have increased quickly. The LoRaWAN (Long-Range Wide Area Network) is one of the most adopted IoT standards in the world [20]. Long-Range (LoRa) technology is generally implemented in the unlicensed 433 MHz and 868 MHz bands, with a channel bandwidth of 125 kHz. The physical layer (PHY) implements a Chirp Spread Spectrum modulation (CSS), which provides excellent robustness against interference [20].

Narrowband Internet of Things (NB-IoT) is a new cellular technology introduced in Third-Generation Partnership Project (3GPP) Release 13 for providing wide-area coverage for IoT. It includes relevant improvements for better performance of IoT applications. Narrowband-IoT (NB-IoT) allows flexibility by using a small portion of the traditional LTE network spectrum [21] requiring 180 kHz of bandwidth for both downlink and uplink. The choice of a minimum system bandwidth enables a number of deployment options (e.g., replacing one GSM carrier (200 kHz) with NB-IoT).

The air interface of NB-IoT is optimized to ensure harmonious coexistence with LTE, and thus such an "in-band" deployment of NB-IoT inside an LTE carrier will not compromise the performance of LTE or NB-IoT. An LTE operator also has the option of deploying NB-IoT in the guard-band of the LTE carrier by upgrading the software of the LTE BS.

3. Methods

3.1. Network Architecture. To implement a dynamic network, we designed a network architecture able to retrieve the required feedback data to the DMT in real time through an IoT feedback loop. Figure 1 shows a block diagram of the proposed network architecture.

The DMT (Block V in Figure 1) collects and analyses Quality of Service (QoS) (Block II, Figure 1) data retrieved from the sensing devices (Block I, Figure 1) to build the REM (Block VI, Figure 1) of the real propagation conditions in the covered area. The QoS data also allows detecting frequencies' interference from secondary services (e.g., adjacent transmitters) and available coverage and taking further actions (Block IV, Figure 1). The actions to take will depend on the scenario that the DMT is working on (e.g., normal conditions or after a disaster caused by a hurricane). In this way, a bridge between the broadcasting network and the DMT network (Block III, Node 1, Node 2, and Node N, Figure 1) was implemented. The

Table 1: Parameters to retrieve by the sensing device at the receiver location.

Parameters	Size	Unit
Channel	7	bit
Frequency offset	10	bit
SNR	7	bit
Bit Error Rate	13	bit
Total	*5*	*Bytes*

IoT network has to be designed and optimized to overlap with the broadcasting network coverage.

To build the sensing device, a Raspberry Pi (RPI), an SDR USB device, and an IoT transceiver were combined (Block I, Figure 1). The RPI has enough computational performance to drive both devices [22]. To detect Digital Terrestrial Multimedia Broadcast (DTMB) signals, the measurement device implemented by hardware using an SDR USB device must accomplish at least with the following parameters: (i) covering the radiofrequency UHF band (470-806MHz), (ii) bandwidth 6 MHz, and (iii) Signal-to-Noise Ratio (SNR) from 14 dB to 30 dB.

Table 1 lists the required parameters to implement the dynamic radiofrequency map and to provide feedback about interference issues to the DMT of Figure 1. The bit size for each parameter is software dependent. The frequency offset is required to correct the local frequency reference and achieve a higher measurement accuracy. A 5-byte packet is sent to the DMT. An IoT transceiver will collect the data packets from the sensing devices and later transmit it to the optimization servers every 5 minutes. Retrieved data is based on the 96-percentile for the previous 5 minutes. For LoRa packets of 10 bytes, the time on air with SF = 7 is around 40 ms [23]. Hence, the latency of the IoT network is not a critical constraint for this application.

3.2. Configuration and Scenario. First, define the proper link budgets for each technology, to sense the broadcasting network and to design and optimize the IoT network. Consider the IoT transceiver and the SDR sensor to be integrated as shown in Figure 1, Block I. Table 2 lists the most relevant link budget parameters for DTMB, SDR sensor, LoRa, and NB-IoT. A link budget accounts for all the gains, losses, and implementation margins in the transmitters, the receiver, and the propagation channel. Based on the link budget, it is possible to calculate the maximum allowable path loss (PLmax) for each technology in a certain scenario [24].

3.3. Broadcasting Network and Hurricane Effects. To make the dynamic map of the radiofrequency spectrum, a realistic suburban scenario in Havana, Cuba, and the currently deployed DTMB network (UHF band) was considered. Three DTMB transmitters (operating on 575 MHz, 677 MHz, and 689 MHz; the last two transmitters are situated in the same building) are covering an area of 50 km^2. Figure 2 shows the coverage area of the broadcast transmitters and available cellular base stations (BSs) (dotted line). To sense the

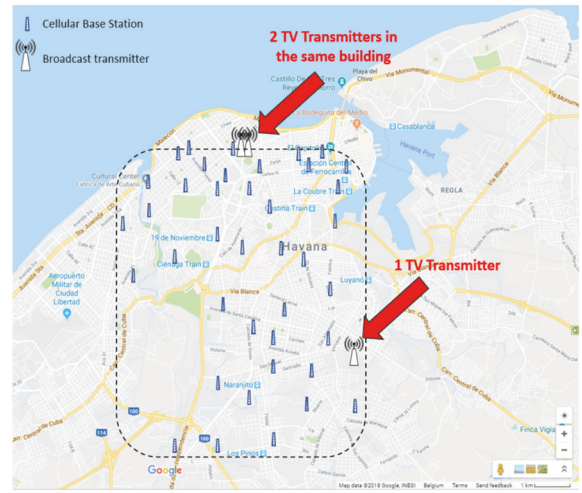

Figure 2: Broadcast transmitters, covered area, and cellular BSs (delimited with dotted line).

radiofrequency spectrum we deploy a number of sensors to cover the area and a number of IoT base stations (BSs) to collect the information from the sensors. The optimization and deployment of the sensors and IoT BSs will be described in Sections 3.5 and 3.6, respectively.

The OFDM parameters (including Frequency Sampling Factor) and bitrate of the broadcast transmitter were retrieved from the DTMB standard specifications [25]. Another specification of the broadcasting network, such as radiated power, radiation efficiency, frequency, bandwidth, antenna parameters, and receiver parameters, depends on the setup, network planning, and technology in use by the service provider (currently deployed network). Notice that the transmitter efficiency takes into consideration both the high-power amplifier and radiation system efficiency.

The shadowing standard deviation was retrieved from the Regulation for Digital Television Broadcast by the local regulatory authorities.

The wind speed in a tropical cyclone in the Caribbean could reach between 250 km/h and 400 km/h (e.g., hurricane Irma in 2017) [26]. The buildings have its structure prepared to support the wind speed, but the cyclone can destroy the windows, knock down the trees, and destroy the electrical service in the area making the circulation almost impossible. Let us suppose that, after the hurricane, two of the three transmitters and approximately 60% of the BSs are destroyed (Figure 3). The TV coverage zone and the operation of the DMT will be affected due to the lack of available infrastructure. The DMT will be helpful to check the spectrum availabilities. Hence, there are two options to get the DMT back: (i) giving priority to the BSs of the cellular network in the recovery process, deploying the DMT using an NB-IoT network, or (ii) deploying a LoRa network without dependencies on the existing or destroyed infrastructure. In both cases, the design of a network redundancy will be taken into account in case the base stations used for the DMT are destroyed by the hurricane.

Table 2: Link budget parameters.

Parameter	DTMB			LoRa	NB-IoT	Unit
Frequency	575	677	689	868	716	MHz
Radiated Power	50	60	58.45	14	23	dBm
Radiation efficiency	16.8	19.6	19.1	15.0	14.6	%
Bandwidth	6			0.125	0.015 0.180	MHz
OFDM Subcarriers	3780			-	12	-
OFDM Used Subcarriers	3744			-	12	-
Frequency Sampling Factor	0.420			0	1.536	-
Cell Interference Margin	0			0	2	dB
BS Antenna Height	40	145	145	20-31	30	m
Receiver Antenna Height	3			3	3	m
Receiver Antenna Gain	8			8	8	dB
Receiver Feeder Losses	0.6			0.6	0.6	dB
Noise Figure	3.5			6	3	dB
Shadowing Standard Deviation	7.5			7.5	7.5	dB
Receiver SNR	35			-20.0 -17.5 -15.0 -12.5 -10.0 -7.5	-12.6 3.0	dB
Bitrate	18274			0.24 0.44 0.97 1.75 3.12 5.46	0.02 204.8	kbps

3.4. IoT Infrastructure. To evaluate the required resources (i.e., infrastructure and spectrum usage) for the IoT feedback loop, we designed, optimized, and compared the two IoT networking solutions in the proposed scenario: LoRa and NB-IoT. Notice that the SigFox constraint of maximum packets delivered per day does not fit this application.

LoRa devices can radiate a signal level higher than 14 dBm (Class A end-devices), but due to the regulation of the maximum allowable radiated power in the 868 MHz, the maximum Equivalent Isotropically Radiated Power (EIRP) is limited to 14 dBm [27]. The maximum EIRP in NB-IoT end-devices is 23 dBm [28].

Using different configurations, LoRa BSs allow emulating up to 49 virtual channels [27]. Here, the maximum available physical channels only are considered (eight channels) [27]. The LoRa PHY layer implements a larger range of modulation schemes, allowing bit rates for a single channel from 0.25 kbps to 5.5 kbps [27]. The SNR is in the range from -7.5 dB to -20 dB. The spread spectrum modulation encodes each bit of information into multiple chirps. Hence, the spread spectrum processing gain allows receiving signal powers below the receiver noise floor.

For NB-IoT, we consider a joint deployment with LTE (band B8-900MHz) BS infrastructure, considering n-band mode. The occupied bandwidth per channel for LoRa is 125 kHz [27], and for NB-IoT is 180 kHz using a single LTE PRB [21]. The radiation efficiency of the NB-IoT power amplifier, radiation system, and the sampling factor will be the same as for LTE [29].

An additional 2 dB loss should be accounted for NB-IoT in the cell interference margin. This is because the LTE cell frequency distribution requires considering a permissible interference among nearby cells [24].

Table 3: The four different categories for sequential design and examples [15].

Input-based	Output-based	Model output-based	Model-based
Uses only input values from previous samples to determine next sample.	Uses input and output values from previous samples to determine next sample.	Uses previous samples and model evaluations to determine next sample	Uses previous samples and model properties and parameters to determine next sample.
Examples: (i) Random sampling (ii) Low-discrepancy sequences (iii) Sequentially nested Latin hypercubes (iv) Voronoi-based sampling (v) Monte Carlo Optimization-based sampling	Examples: (i) LOLA-Voronoi	Examples: (i) Adaptation to irregularities (ii) Slope, local optima and variance criteria (iii) Sequential Exploratory Experimental Design method (SEED) (iv) Model error sampling	Examples: (i) Kriging-based

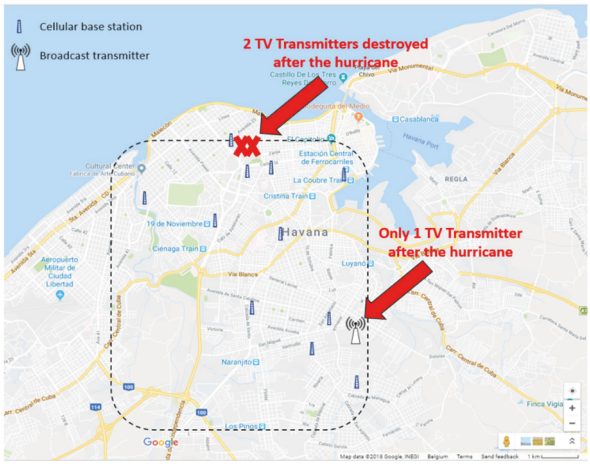

Figure 3: Broadcast transmitters, covered area, and cellular BSs (delimited with dotted line) after some meteorological event.

3.5. Sensing Network Optimizations. To optimize the sensing networks, several parameters need to be taken into account. Firstly, we have to cover an area of 50 km^2 in a suburban area with three TV transmitters working in the UHF band (470-806MHz). Hence, the propagation loss plays an important role at the moment to decide how many sensors we are going to use. To estimate its behavior, the Okumura-Hata model for propagation loss in a suburban scenario is considered, which is fully explained in [30].

Secondly, we have to calculate the required number of sensors to fit the area avoiding the errors trying to estimate the received power among adjacent sensors. To achieve that, the received power was estimated using the Okumura-Hata model in a suburban area varying the receiving distance in steps of 1 km. Figure 5 shows the results for the three transmitters in the area.

As can be seen, the received power drops dramatically in the first 10 km for all the transmitters. However, for the 575 MHz frequency and transmitted power of 50 dBm, after 5 km the received power drops under the TV sensitivity threshold established in a Cuban regulation for UHF band (-84 dBm) [31]. Hence, the proposition is to work with a resolution of one sensor per km^2.

To optimize the deployment the SUMO was used [32, 33]. The SUMO is a MATLAB tool that automatically builds accurate surrogate models (also known as meta-models or response surface models) of a given data source (simulation code, dataset, script, etc.) within the accuracy and time constraints set by the user. The tool minimizes the number of data points (which it chooses automatically) and tries to be as adaptive and autonomous as possible, requiring no user input besides some initial configuration [32, 33].

Usually, the simulations require expensive computational hardware. Hence, the SUMO tool is an alternative to deeply explore the design space by evaluating large amounts of samples. The goal of surrogate modeling is to find a model that mimics the original system's behavior but can be evaluated much faster. This function is constructed by calculating multiple samples at key points in the design space, analyzing the results, and selecting a model that approximates the samples and the system behavior.

Table 3 shows a wide variety of model types available; their limitations depend on the system that is being modeled. Popular choices are polynomial and rational functions [34], Kriging models [35], neural networks [36], and radial basis function (RBF) models [37]. These can be used to perform optimization and sensitivity analysis once the model is constructed [38].

Also, the SED [11, 39] was used trying to achieve a similar result and thus compare both deployments. The SED is a powerful tool for sequential Design of Experiments (DoE). In traditional experimental design, all the design points are selected up front, before performing any (computer or real-life) experiment, and no additional design points are selected afterward. This traditional approach is prone to oversampling and/or undersampling because it is often very

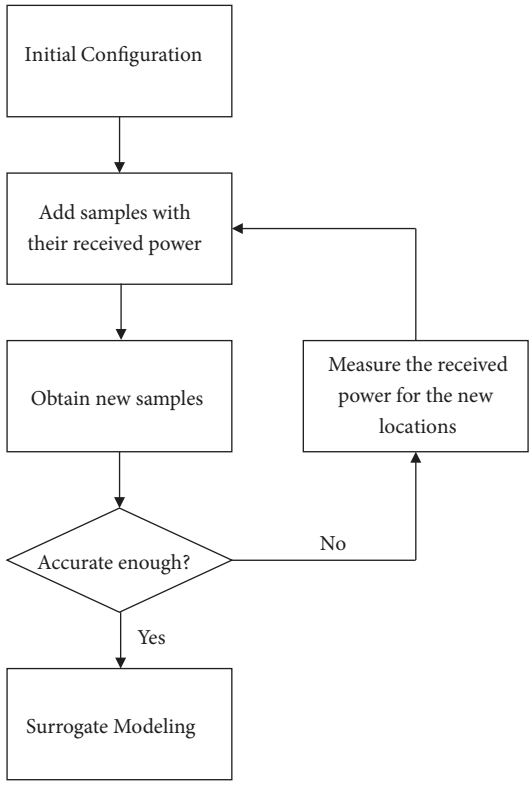

Figure 4: Flow diagram of the Sequential Design, including the SUrrogate MOdeling.

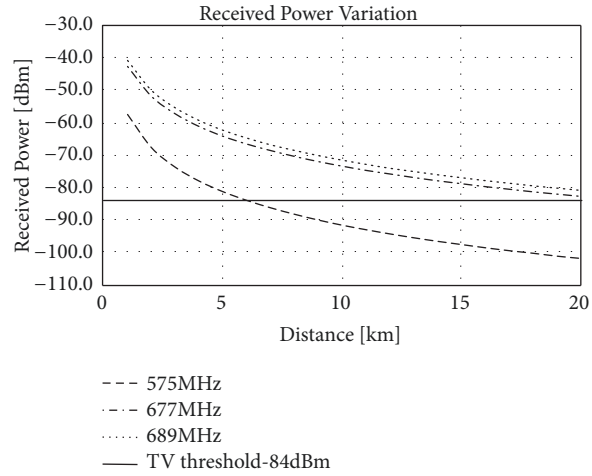

Figure 5: Received power variation using the Okumura-Hata model in steps of 1 km. The inputs parameters were taken from Table 2.

difficult to estimate the required number of design points in advance. The SED tool solves this problem by providing the user with state-of-the-art algorithms that generate an experimental design in a sequential way, i.e., one point at a time, without having to provide the total number of design points in advance. The SED was designed to be extremely fast and easy to use, yet very powerful [11, 39].

The traditional DoE is chosen based only on the available information in the first simulation, such as the input variables and the result of the measurements. This information is then added to the experimental design in the simulator, which evaluates all the information in the Surrogate Model. This is a one-shot run, where all the points are assessed at once, and the modeling algorithm proceeds without evaluating any additional samples [40].

Sequential Experimental Design (SED) improves on this approach by transforming the unique algorithm into an iterative process. SED methods analyze data (samples) and models from previous iterations to select new samples in areas that are more difficult to approximate, resulting in a more efficient distribution of samples compared to the traditional DoE.

Figure 4 shows the flow graph to work with both tools (SUMO and SED). In the first step (initial configuration), the coordinates (UMT format to SUMO tool and degree format to SED tool) of the area under evaluation need to be added. In addition, constraints are defined with, e.g., buildings, lakes, or rivers, not allowed areas to place the sensors. In both tools, these are known as "constraints." Finally, the number of samples to add in every iteration and the final number of samples to deploy need to be assigned. The rest of the process continues with a loop until finding the optimal number of sensors to deploy is defined. In the case of the SUMO tool, it starts adding known samples with their received power (dBm). If the number of samples does not satisfy the requirements, the tool advises new locations (samples), where the received power should be measured. There are then new samples and the whole process is repeated again. In the case of SED, putting the desired number of sensors to deploy is only needed and it will design the whole deployment.

Table 3 lists some of the available methods to work with SUMO and SED tools. A model is considered accurate enough when its root relative square error is lower than 0.05 [8]. The maximum number of samples allowed for each frequency was fixed at 65. In this paper, the output-based (LOLA-Voronoi) and model-based (Kriging-based) sampling were used because both use the input and output values from previous samples to determine the next samples. By adding samples after every simulation, the REM can be built as precisely as we want.

3.6. IoT Networks Optimizations. To optimize the IoT network, the power consumption of the dedicated feedback channel has to be minimized. To this aim, an IoT LoRa and an NB-IoT network (Table 2) are designed, optimized, and benchmarked.

To account for the minimally required infrastructure and optimize the network power consumption, the heuristic algorithm presented in [41, 42] and improved in [1] was used to reduce the number of base stations required in the IoT physical layer. Figure 6 shows the process for the design and optimization for minimal infrastructure and power consumption of the IoT feedback network. The design and the optimization are performed in two different steps (two heuristic cycles of the algorithm). In the original algorithm

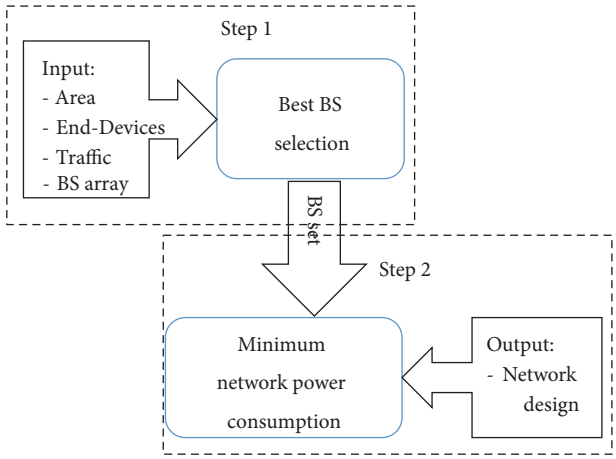

Figure 6: IoT network optimization process.

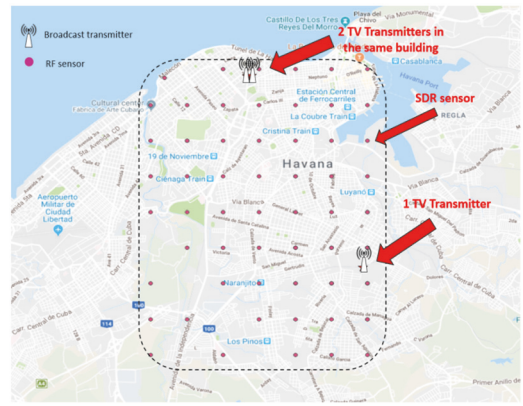

Figure 7: Sensing network deployment for the UHF band using SUMO and SED for optimal positioning and number of sensors for spectrum monitoring.

presented in [11, 41], only one cycle is present (no optimal BS location selection is implemented). The network design tool is capacity-based, meaning that the traffic density and end-devices density are input parameters. The software also receives as input parameters the target area and a number of possible BS geo-locations including the BS antenna height. Forty simulations are performed to assess the mean power consumption of the whole network, where the progressive average for all simulations is calculated to validate a proper estimation of the percentage of users covered.

In the first step (Figure 6), the best set of BSs among the whole set of possible BS locations is chosen. Forty-one available BS locations were considered in the scenario of Section 3.2. The software optimizes the power consumption connecting each user to the active BS with the lowest path loss if this BS still has enough capacity to support the user. Only if no other active BS can support the current end-device, then a new BS is marked as active.

The best BS locations in terms of path loss are statistically chosen after 40 simulations (step 1). The maximum number of BSs chosen will depend on the traffic demand and effective coverage per BS that guarantee at least 96% of end-devices actually covered by the network. The Path Loss (PL) [dB] between the end-devices and each base station (BS) is calculated as a function of the distance d [km], the frequency f [MHz], the BS antenna height hb [m], and the end-device antenna height hm [m]. For our scenario, we use the Okumura-Hata path loss model [30], which fits well with the scenario topology and related technology parameters (i.e., frequency, maximum range, and effective heights).

In the second step of the algorithm (Figure 6), the power consumption is further optimized by connecting users to the active BSs with the lowest path loss and by reducing the EIRP while the PL between the base station and end-devices is less than the maximum PL.

4. Results and Discussion

This section presents the results of the network simulations and optimizations in the considered scenario.

4.1. Sensing Network Optimization. As mentioned in Section 3.5, we calculated the optimal position for sensors using SUMO and SED tools. The main constraint of both tools is that they use approximation algorithms. As a result, we will obtain a new deployment every time we run the application (number and position of the sensors might be different) until the optimal position is found.

In order to improve the accuracy, an adaptive sampling procedure drives the selection and simulation of new samples. Modeling starts with 30 known samples using LOLA-Voronoi. Afterwards, a Kriging-based model adaptive sampling is applied. After each sampling iteration, 10 more samples are required, the received power (in dBm) for every new sample is estimated, and the process is repeated until one of the following conditions [9] is satisfied: (i) the user required accuracy has been achieved and (ii) the maximum allowed number of samples has been reached.

Once the 65 samples for each frequency (one per transmitter) are obtained, the results should be combined to obtain the final deployment, with the condition of every sensor having to receive information from the three available transmitters in the selected zone. The difference among sensors is fairly small to assume one final position for the same sensor. Only seven more sensors were required to cover the entire area. Finally, an optimal deployment of 72 sensors in the selected area was obtained. Figure 7 shows the sensors' deployment in the selected area.

Figure 8 shows the coverage zone for the three transmitters in the area. Figure 8(a) represents the coverage zone for the transmitter working on 575 MHz. It does not cover the entire zone (50 dBm of radiated power and 40 m of antenna height) because the received power in some parts of the selected area is under the TV sensitivity threshold for UHF band (-84 dBm). However, the other two transmitters transmitting on 677 MHz (Figure 8(b)) and 689 MHz (Figure 7c) located in the same building (60 dBm and 58.45 dBm, respectively, of radiated power and 145 m of antenna height) can cover the selected area without reaching the TV sensitivity threshold (-84 dBm) in any part of the area.

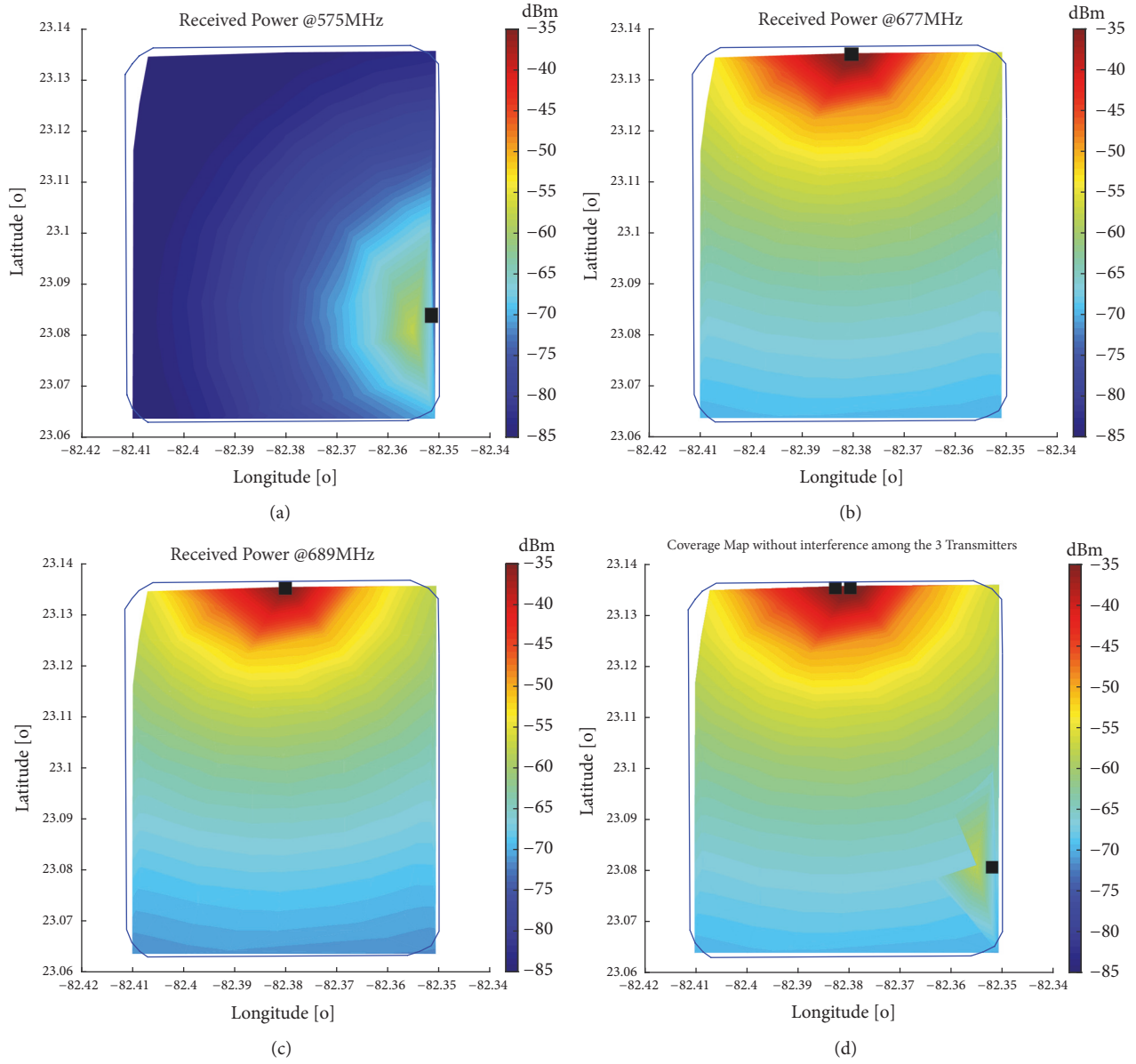

FIGURE 8: Coverage map simulation-based in the selected area, (a) 575 MHz, (b) 677 MHz, (c) 689 MHz, and (d) coverage map with the 3 transmitters (black square) working in the area without interference among them.

Every one of those transmitters is working at a different frequency and transmitting different information. Hence, there is no interference between them. Figure 8(d) shows the three transmitters together; 100 percent of the area is covered by the TV signal with a received power higher than -84 dBm in every point.

4.2. IoT Feedback Network Optimization. Figure 9 shows the two obtained solutions for the IoT feedback network coverage map in the considered area, for LoRa (Figure 9(a)) and NB-IoT (Figure 9(b)), using the method and scenarios of Section 3.2. The BSs chosen to optimally satisfy the density of connected devices and traffic are highlighted with a darker color.

The required number of BSs for LoRa is 4 and for NB-IoT is 6. Theoretically, the area coverage requirement (50 km^2) is satisfied with only 1 to 3 BSs (depending on the SF). However, a larger number of BSs are required to satisfy the capacity demand for the worst-case traffic generated by the monitoring application of the receivers. For this reason, the best LoRa network performance is achieved if all devices are capable of connecting with SF=7 to the nearest BS (in terms of path loss). The reason for this is that SF=7 achieves the highest bit rate and lowest time on air. NB-IoT has a higher capacity with QPSK modulation scheme, but the maximum coverage per BS (i.e., ~2 km) is lower than LoRa SF=7 (i.e., ~3.1 km).

Notice that the DMT will be deployed using the existing infrastructure to provide 3G and in a near feature LTE. In our

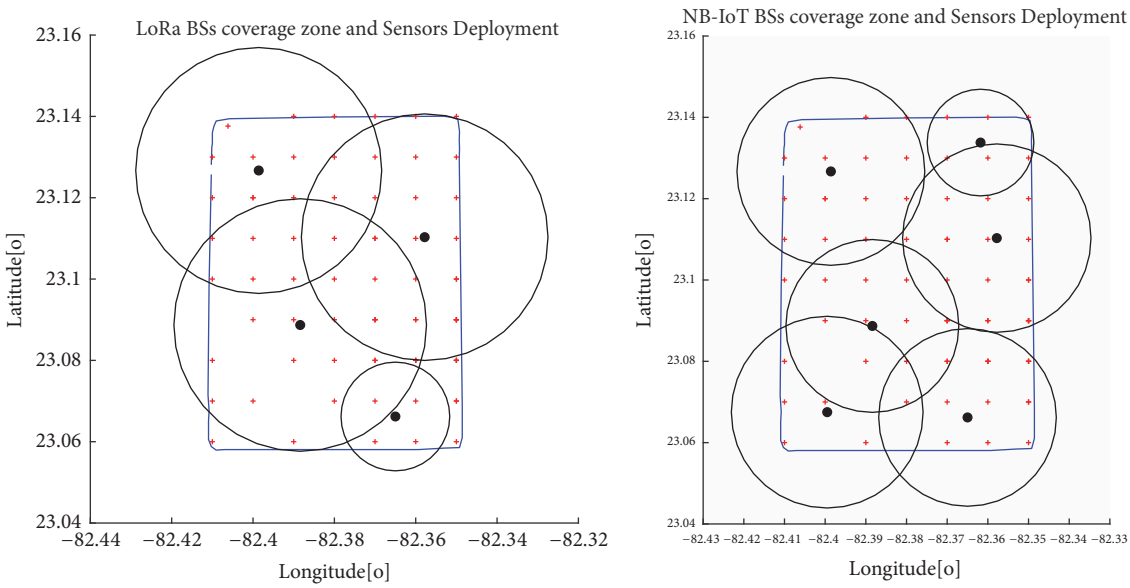

Figure 9: IoT feedback network coverage map (black circles): selected BS locations (black points) and sensors with red crosses, (a) LoRa network solution and (b) NB-IoT network solution.

solutions (LoRa and NB-IoT) more than 70% of the possible BS locations are never chosen. As such, the algorithm is a heuristic: the obtained solution might not be (nevertheless, it can be) the optimal solution, but it is a suboptimal one close to the optimal one. The approach that more than 70% of possible BSs are never chosen can be used to develop a background network to face the recovering process after a meteorological event. Removing the chosen BSs in the previous design and running the described process in Figure 6, a new optimal deployment is obtained.

4.3. Recovery Process after a Meteorological Event. The scenario presented in Section 3.2, where it is assumed that two of the three transmitters are destroyed by the hurricane, is considered. These two transmitters are located on the same building with a height of 145 m retrieving in a higher probability of the antenna destruction caused by the wind. The process to recover the original transmitters can take days and during this time, the people in the area are still uninformed about the situation they are facing.

In this case, the proposed DMT plays an important role in helping the authorities during the recovery process after a disaster event. The first step to keep the DMT running is to provide the sensing devices with batteries (Figure 1, Block I). The Raspberry PI is the core of the sensing device and it works with 5V consuming around 2A. Hence, with a power bank of 10,000 mAh, the sensing devices run around 5 hours.

The second step is to have all the necessary base stations working to collect the information from the sensing devices. In Section 4.2, we provided two solutions. The first uses 4 LoRa BSs and the second one uses 6 NB-IoT BSs. All these locations are used to provide cellular connections and are equipped with a backup power supply and cooling system, making them work during and after the hurricane. To decide the best solution, the following elements need to be accounted for: (i) access level to those locations after the hurricane, (ii) BSs' state, and (iii) in case of partial or total destruction how much time it takes to restore the service. The IoT technology will be chosen depending on the elements previously mentioned.

As mentioned, we obtained two solutions for the IoT network: 4 BSs for LoRa and 6 BSs for NB-IoT. The locations of LoRa BSs coincide in position with 4 of the 6 locations of NB-IoT BSs. However, the antennas of both technologies use the same tower. Hence, the time to repair one tower is the same no matter the technology. To have the DMT working back and save time in the recovery process, it is better to use LoRa solution.

For the scenario described in Section 3.3 where two transmitters were destroyed, the one still transmitting does not have enough power to cover the entire area (Figure 8(a)). The DMT can detect that in approximately 30% of the area the received power is under -84 dBm. In this situation and to keep the people informed, we propose using a small transmitter located in the same building with a transmission power of 40 W (around $700) instead of repairing the original one (installation time will be longer and price will be higher, around $20,000). Figure 10(a) shows the coverage area of the new transmitter (~46 dBm, 145 m of antenna height). Figure 10(b) shows the two transmitters together and 90% of the area is covered by the TV signal with a signal strength higher than -84 dBm. Only 10% (black square) of the area still remains as an unserved area.

In Section 3.3, we assumed that 60% of the 41 available base stations we needed to provide a cellular connection

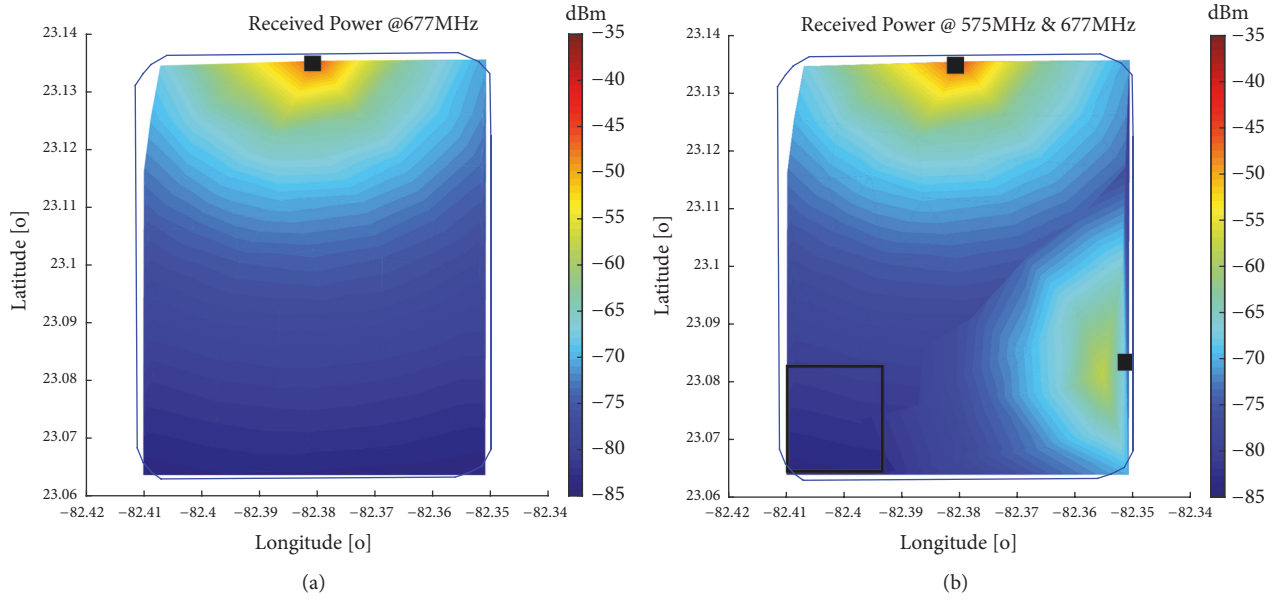

FIGURE 10: Coverage map (received-power) simulation-based in the selected area, (a) 677 MHz with a transmitted power of 40 W, (b) coverage map with the 2 transmitters (black square) working in the area without interference between them. The black square is the unserved area, around 10% of the total surface.

(GSM, 3G, and 4G) were destroyed by the hurricane (25 BSs destroyed). After a hurricane, it is difficult to check all the BSs in a short time period. In this situation, the proposed DMT is useful to precisely detect which BS is working and give the authorities feedback about the real situation.

4.4. Network Deployment Cost Considerations. For network deployment, we need to consider the end-devices structure and the BS infrastructure. A single sensing device is built with an SDRplay sensor (model RSP1A), a Raspberry PI 3 (model B+), and an IoT transceiver (LoRa and NB-IoT). The approximate price for all of these devices is $215. The total price for 72 sensors is approximately $15,480. A single LoRa BS has deployment cost up to $1,000 and a single NB-IoT of $15,000, considering the reusage of LTE infrastructure. The difference in infrastructure is not significant (2 BSs more for NB-IoT). However, the NB-IoT license cost for the mobile operator is thus considerably higher. The total LoRa BSs infrastructure cost is just $4,000 (4 BSs). For NB-IoT, the total BSs deployment cost is $90,000 (approximately 22 times higher for 6 BSs).

5. Conclusion

In this paper, we investigated the feasibility of building a REM deploying 72 SDR sensors using SUMO and SED tool in a selected area and using LoRa and/or NB-IoT technologies for networking. The IoT feedback network is designed and optimized for minimal power consumption and infrastructure.

This DMT permits the regulatory body to check the correct use of the assigned spectrum and plays an important role in the recovery process after a catastrophic event, such as a hurricane, where radio and TV broadcasting are important in keeping people informed. Besides, the tool can be used to deploy new services in the nonserved area (e.g., 4G in the 700 MHz).

Future research will consist of the emulation of the DMT in a real scenario.

Data Availability

The data used to support the findings of this study are available from the corresponding author upon request.

Disclosure

M. Deruyck is a Postdoctoral Fellow of the FWO-V (Research Foundation, Flanders, Belgium).

Conflicts of Interest

The authors declare that there are no conflicts of interest regarding the publication of this paper.

Acknowledgments

Y. Hervis Santana is supported by *LACETEL* and a doctoral grant from the Special Research Fund (BOF) of Ghent University, Belgium.

References

[1] R. M. Alonso et al., "IoT-Based Management Platform for Real-Time Spectrum and Energy Optimization of Broadcasting

Networks," *Wireless Communications and Mobile Computing*, vol. 2018, 2018.

[2] V. Popescu, M. Fadda, M. Murroni, J. Morgade, and P. Angueira, "Co-channel and adjacent channel interference and protection issues for DVB-T2 and IEEE 802.22 WRAN operation," *IEEE Transactions on Broadcasting*, vol. 60, no. 4, pp. 693–700, 2014.

[3] M. Kosunen, V. Turunen, K. Kokkinen, and J. Ryynanen, "Survey and Analysis of Cyclostationary Signal Detector Implementations on FPGA," *IEEE Journal on Emerging and Selected Topics in Circuits and Systems*, vol. 3, no. 4, pp. 541–551, 2013.

[4] Z. Quan, S. Cui, and A. H. Sayed, "Optimal Linear Cooperation for Spectrum Sensing in Cognitive Radio Networks," *IEEE Journal of Selected Topics in Signal Processing*, vol. 2, no. 1, pp. 28–40, 2008.

[5] D. Sinha, A. K. Verma, and S. Kumar, "Software defined radio: Operation, challenges and possible solutions," in *Proceedings of the 2016 10th International Conference on Intelligent Systems and Control (ISCO)*, pp. 1–5, 2016.

[6] M. B. Sruthi, M. Abirami, A. Manikkoth, R. Gandhiraj, and K. P. Soman, "Low cost digital transceiver design for software defined radio using RTL-SDR," in *Proceedings of the 2013 International Mutli-Conference on Automation, Computing, Communication, Control and Compressed Sensing (iMac4s)*, pp. 852–855, 2013.

[7] N. LLC, "Nuand — bladeRF Software Defined Radio," http://www.nuand.com, Accessed: 03-Dec-2018.

[8] L. De Tommasi, D. Gorissen, J. A. Croon, and T. Dhaene, "Surrogate Modeling of RF Circuit Blocks," *Mathematics in Industry*, vol. 15, pp. 2–7, 2010.

[9] L. De Tommasi, D. Gorissen, J. Croon, and T. Dhaene, "Surrogate Modeling of Low Noise Amplifiers Based on Transistor Level Simulations," *Scientific Computing in Electrical Engineering*, vol. 14, pp. 225–232, 2010.

[10] K. Crombecq, I. Couckuyt, D. Gorissen, and T. Dhaene, "Space-filling sequential design strategies for adaptive surrogate modelling," in *Proceedings of the First International Conference on Soft Computing Technology in Civil, Structural and Environmental Engineering, B.H.V*, 2009.

[11] K. Crombecq, L. De Tommasi, D. Gorissen, and T. Dhaene, "A novel sequential design strategy for global surrogate modeling," in *Proceedings of the 2009 Winter Simulation Conference, WSC*, pp. 731–742, 2009.

[12] S. Srinu, S. L. Sabat, and S. K. Udgata, "FPGA implementation of cooperative spectrum sensing for cognitive radio networks," in *Proceedings of the 2010 Second UK-India-IDRC International Workshop on Cognitive Wireless Systems (UKIWCWS)*, pp. 1–5, 2010.

[13] A. Sahai, N. Hoven, and R. Tandra, "Some Fundamental Limits on Cognitive Radio," in *Proceedings of the Allert. Conf. Control. Commun. Comput*, pp. 1662–1671, 2004.

[14] H. Birkan Yilmaz, T. Tugcu, and F. Alagoz, "Novel quantization-based spectrum sensing scheme under imperfect reporting channel and false reports," *International Journal of Communication Systems*, vol. 27, no. 10, pp. 1459–1475, 2014.

[15] K. Crombecq, *Surrogate Modeling of Computer Experiments with Sequential Experimental Design*, Universiteit Antwerpen, 2011.

[16] R. Martin and R. Thomas, "Algorithms and bounds for estimating location, directionality, and environmental parameters of primary spectrum users," *IEEE Transactions on Wireless Communications*, vol. 8, no. 11, pp. 5692–5701, 2009.

[17] J. A. Bazerque and G. B. Giannakis, "Distributed spectrum sensing for cognitive radio networks by exploiting sparsity," *IEEE Transactions on Signal Processing*, vol. 58, no. 3, pp. 1847–1862, 2010.

[18] Y. Zhao, J. Gaeddert, K. K. Bae, and J. H. Reed, "Radio Environment Map Enabled Situation-Aware Cognitive Radio Learning Algorithms," in *Proceedings of the Tech. Conf. Prod. Expo*, 2006.

[19] H. Yilmaz Birkan, T. Tugcu, F. Alagöz, and S. Bayhan, "Radio environment map as enabler for practical cognitive radio networks," *IEEE Communications Magazine*, vol. 51, no. 12, pp. 162–169, 2013.

[20] R. S. Sinha, Y. Wei, and S.-H. Hwang, "A survey on LPWA technology: LoRa and NB-IoT," *ScienceDirect*, vol. 3, no. 1, pp. 14–21, 2017.

[21] Y. E. Wang, X. Lin, A. Adhikary et al., "A Primer on 3GPP Narrowband Internet of Things," *IEEE Communications Magazine*, vol. 55, no. 3, pp. 117–123, 2017.

[22] D. Ball, N. Naik, and P. Jenkins, "Lightweight and Cost-Effective Spectrum Analyser Based on Software Defined Radio and Raspberry Pi," in *Proceedings of the 2017 European Modelling Symposium (EMS)*, pp. 260–266, 2017.

[23] F. Adelantado, X. Vilajosana, P. Tuset-Peiro, B. Martinez, J. Melia-Segui, and T. Watteyne, "Understanding the Limits of LoRaWAN," *IEEE Communications Magazine*, vol. 55, no. 9, pp. 34–40, 2017.

[24] M. Deruyck, E. Tanghe, W. Joseph, and L. Martens, "Modelling and optimization of power consumption in wireless access networks," *Computer Communications*, vol. 34, no. 17, pp. 2036–2046, 2011.

[25] "S. A. of the P. Republic and China, "GB20600-2006 Standard: Framing Structure, Channel Coding and Modulation for Digital Television Terrestrial Broadcasting System (DTMB),"," 2006.

[26] "Cuba después del huracán Irma: Últimas noticias y testimonios III (miércoles 13 de septiembre) — Cubadebate," http://www.cubadebate.cu/temas/politica-temas/2017/09/13/cuba-despues-del-huracan-irma-ultimas-noticias-y-testimonios-iii/#.XAZ-_GhKi-Uk, 2017, Accessed: 04-Dec-2018.

[27] T. Rheinland, *A technical overview of LoRa® and LoRaWAN™ What is it?*, 2015.

[28] 3GPP, *Cellular System Support for Ultra Low Complexity and Low Throughput Internet of Things*, Valbonne-France, 2015, Release 13.

[29] L. Zhang, A. Ijaz, P. Xiao, and R. Tafazolli, "Channel Equalization and Interference Analysis for Uplink Narrowband Internet of Things (NB-IoT)," *IEEE Communications Letters*, vol. 21, no. 10, pp. 2206–2209, 2017.

[30] A. F. Molish and Fellow IEEE, *Wireless Communications*, Calif, USA, 2nd edition, 2011.

[31] "Mi. de Comunicaciones," RESOLUCIÓN No. 124 /2016. Cuba, 2016, p. 11.

[32] D. Gorissen, I. Couckuyt, P. Dhaene, and T. Demeester, "A Surrogate Modeling and Adaptive Sampling Toolbox for Computer Based," 2010.

[33] J. van der Herten, I. Couckuyt, D. Deschrijver, and T. Dhaene, "Adaptive classification under computational budget constraints using sequential data gathering," *Advances in Engineering Software*, vol. 99, pp. 137–146, 2016.

[34] D. Deschrijver, T. Dhaene, and J. Broeckhove, "Adaptive model based parameter estimation, based on sparse data and frequency derivatives," in *Proceedings of the International Conference on Computational Science*, pp. 443–450, 2004.

[35] W. C. M. Van Beers, "Kriging metamodeling in discrete-event simulation: An overview," in *Proceedings of the 2005 Winter Simulation Conference*, p. 2, 2005.

[36] L. Balewski and M. Mrozowski, "Creating neural models using an adaptive algorithm for optimal size of neural network and training set," in *Proceedings of the 15th International Conference on Microwaves, Radar and Wireless Communications*, vol. 2, pp. 543–546, IEEE Cat. No.04EX824.

[37] A. Lamecki, P. Kozakowski, and M. Mrozowski, "CAD-model construction based on adaptive radial basis functions interpolation technique," in *Proceedings of the 15th International Conference on Microwaves, Radar and Wireless Communications, MIKON - 2004*, pp. 799–802, IEEE Cat. No.04EX824, 2004.

[38] H. Zhao, D. Knight, E. Taskinoglu, and V. Jovanovic, "Data driven design optimization methodology development and application," in *Proceedings of the International Conference on Computational Science (LNCS 3038)*, pp. 748–755, 2004.

[39] K. Crombecq and T. Dhaene, *Generating Sequential Space-filling Designs Using Genetic Algorithms and Monte Carlo Methods*, 2010.

[40] K. Crombecq, E. Laermans, and T. Dhaene, "Efficient space-filling and non-collapsing sequential design strategies for simulation-based modeling," *European Journal of Operational Research*, vol. 214, no. 3, pp. 683–696, 2011.

[41] M. Deruyck, J. Wyckmans, L. Martens, and W. Joseph, "Emergency ad-hoc networks by using drone mounted base stations for a disaster scenario," in *Proceedings of the 12th IEEE International Conference on Wireless and Mobile Computing, Networking and Communications, WiMob*, pp. 1–7, 2016.

[42] R. Martinez Alonso, D. Plets, M. Deruyck, L. Martens, G. Guillen Nieto, and W. Joseph, "TV white space and LTE network optimization toward energy efficiency in suburban and rural scenarios," *IEEE Transactions on Broadcasting*, vol. 64, no. 1, pp. 164–171, 2018.